SOLAR NEUTRINOS

Revised September 2001 by K. Nakamura (KEK, High Energy Accelerator Research Organization, Japan).

1. Introduction: The Sun is a main-sequence star at a stage of stable hydrogen burning. It produces an intense flux of electron neutrinos as a consequence of nuclear fusion reactions whose combined effect is

$$4p \rightarrow {}^4\mathrm{He} + 2e^+ + 2\nu_e \ . \tag{1}$$

Positrons annihilate with electrons. Therefore, when considering the solar thermal energy generation, a relevant expression is

$$4p + 2e^- \rightarrow {}^4\mathrm{He} + 2\nu_e + 26.73 \text{ MeV} - E_\nu \ , \tag{2}$$

where E_ν represents the energy taken away by neutrinos, with an average value being $\langle E_\nu \rangle \sim 0.6$ MeV. The neutrino-producing reactions which are at work inside the Sun are enumerated in the first column in Table 1. The second column in Table 1 shows abbreviation of these reactions. The energy spectrum of each reaction is shown in Fig. 1.

A pioneering solar neutrino experiment by Davis and collaborators using ^{37}Cl started in the late 1960's. Since then, chlorine and gallium radiochemical experiments and water Cherenkov experiments with light and heavy water targets have made successful solar-neutrino observations.

Observation of solar neutrinos directly addresses the theory of stellar structure and evolution, which is the basis of the standard solar model (SSM). The Sun as a well-defined neutrino source also provides extremely important opportunities to investigate nontrivial neutrino properties such as nonzero mass and mixing, because of the wide range of matter density and the very long distance from the Sun to the Earth.

From the very beginning of the solar-neutrino observation, it was recognized that the observed flux was significantly smaller than the SSM prediction provided nothing happens to the electron neutrinos after they are created in the solar interior. This deficit has been called "the solar-neutrino problem." The recent result from Sudbury Neutrino Observatory (SNO) on

the solar neutrino flux measured via charged-current reaction $\nu_e d \rightarrow e^- pp$, combined with the Super-Kamiokande's high-statistics flux measurement via νe elastic scattering, provided direct evidence for flavor conversion of solar neutrinos. The most probable explanation is neutrino oscillation which can also solve the solar-neutrino problem.

2. Solar Model Predictions: A standard solar model is based on the standard theory of stellar evolution. A variety of input information is needed in the evolutionary calculations. The most elaborate SSM, BP2000 [1], is presented by Bahcall et al. who define their SSM as the solar model which is constructed with the best available physics and input data. Though they used no helioseismological constraints in defining the SSM, the calculated sound speed as a function of the solar radius shows an excellent agreement with the helioseismologically determined sound speed to a precision of 0.1% rms throughout essentially the entire Sun. This greatly strengthen confidence in the solar model. The BP2000 prediction [1] for the flux, contributions to the event rates in chlorine and gallium solar-neutrino experiments from each neutrino-producing reaction is listed in Table 1. The solar-neutrino spectra shown in Fig. 1 also resulted from the BP2000 calculations [1].

Another recent solar-model predictions for solar-neutrino fluxes were given by Turck-Chieze et al. [2] Their model is based on the standard theory of stellar evolution where the best physics available is adopted, but some fundamental inputs such as the p-p reaction rate and the heavy-element abundance in the Sun are seismically adjusted within the commonly estimated errors aiming at reducing the residual differences between the helioseismologically-determined and the model-calculated sound speeds. Their predictions for the event rates in chlorine and gallium solar-neutrino experiments as well as ^{8}B solar-neutrino flux are shown in the last line in Table 2, where the BP2000 predictions [1] are also shown in the same format. As is apparent from this table, the predictions of the two models are remarkably consistent.

Table 1: Neutrino-producing reactions in the Sun (the first column) and their abbreviations (second column). The neutrino fluxes and event rates in chlorine and gallium solar-neutrino experiments predicted by Bahcall, Pinsonneault, and Basu [1] are listed in the third, fourth, and fifth columns respectively.

		BP2000 [1]		
Reaction	Abbr.	Flux (cm^{-2} s^{-1})	Cl (SNU*)	Ga (SNU*)
$pp \rightarrow d\,e^+\,\nu$	pp	$5.95(1.00^{+0.01}_{-0.01}) \times 10^{10}$	—	69.7
$pe^-p \rightarrow d\,\nu$	pep	$1.40(1.00^{+0.015}_{-0.015}) \times 10^{8}$	0.22	2.8
^{3}He $p \rightarrow {}^4$He $e^+\nu$	hep	9.3×10^3	0.04	0.1
^{7}Be $e^- \rightarrow {}^7$Li $\nu + (\gamma)$	^{7}Be	$4.77(1.00^{+0.10}_{-0.10}) \times 10^{9}$	1.15	34.2
^{8}B $\rightarrow {}^8$Be* $e^+\nu$	^{8}B	$5.05(1.00^{+0.20}_{-0.16}) \times 10^{6}$	5.76	12.1
^{13}N $\rightarrow {}^{13}$C $e^+\nu$	^{13}N	$5.48(1.00^{+0.21}_{-0.17}) \times 10^{8}$	0.09	3.4
^{15}O $\rightarrow {}^{15}$N $e^+\nu$	^{15}O	$4.80(1.00^{+0.25}_{-0.19}) \times 10^{8}$	0.33	5.5
^{17}F $\rightarrow {}^{17}$O $e^+\nu$	^{17}F	$5.63(1.00^{+0.25}_{-0.25}) \times 10^{6}$	0.0	0.1
Total			$7.6^{+1.3}_{-1.1}$	128^{+9}_{-7}

* 1 SNU (Solar Neutrino Unit) = 10^{-36} captures per atom per second.

3. Solar Neutrino Experiments: So far, seven solar-neutrino experiments have published results. The most recent published results on the average event rates or flux from these experiments are listed in Table 2 and compared to the two recent solar-model predictions.

3.1. Radiochemical Experiments: Radiochemical experiments exploit electron neutrino absorption on nuclei followed by their decay through orbital electron capture. Produced Auger electrons are counted.

The Homestake chlorine experiment in USA uses the reaction

$$^{37}\mathrm{Cl} + \nu_e \rightarrow {}^{37}\mathrm{Ar} + e^- \ \text{(threshold 814 keV)} \ . \qquad (3)$$

Three gallium experiments (GALLEX and GNO at Gran Sasso in Italy and SAGE at Baksan in Russia) use the reaction

$$^{71}\mathrm{Ga} + \nu_e \rightarrow {}^{71}\mathrm{Ge} + e^- \ \text{(threshold 233 keV)} \ . \qquad (4)$$

The produced ^{37}Ar and ^{71}Ge atoms are both radioactive, with half lives ($\tau_{1/2}$) of 34.8 days and 11.43 days, respectively. After an exposure of the detector for two to three times $\tau_{1/2}$, the

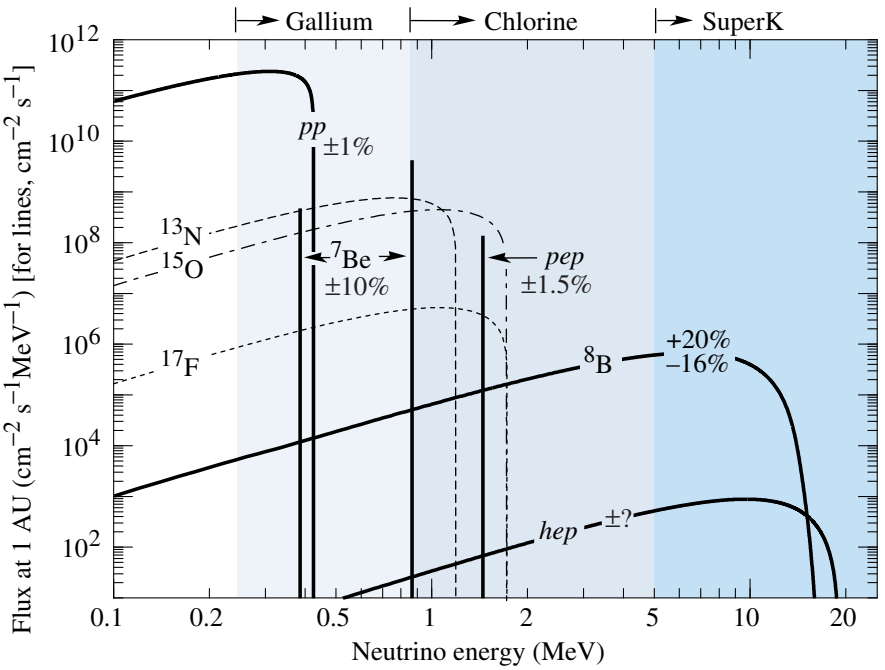

Figure 1: The solar neutrino spectrum predicted by the standard solar model. The neutrino fluxes from continuum sources are given in units of number $cm^{-2}s^{-1}MeV^{-1}$ at one astronomical unit, and the line fluxes are given in number $cm^{-2}s^{-1}$. Spectra for the *pp* chain, shown by the solid curves, are courtesy of J.N. Bahcall (2001). Spectra for the CNO chain are shown by the dotted curves, and are also courtesy of J.N. Bahcall (2001).

reaction products are chemically extracted and introduced into a low-background proportional counter, and are counted for a sufficiently long period to determine the exponentially decaying signal and a constant background.

Solar-model calculations predict that the dominant contribution in the chlorine experiment comes from ^{8}B neutrinos, but ^{7}Be, *pep*, ^{13}N, and ^{15}O neutrinos also contribute. At present, the most abundant *pp* neutrinos can be detected only in gallium experiments. Even so, according to the solar-model calculations almost half of the capture rate in the gallium experiments is due to other solar neutrinos.

Table 2: Recent results from the seven solar-neutrino experiments and a comparison with standard solar-model predictions. Solar model calculations are also presented. The first and the second errors in the experimental results are the statistical and systematic errors, respectively. The third error in the SNO result is the charged-current cross-section uncertainty.

	$^{37}\mathrm{Cl}\rightarrow^{37}\mathrm{Ar}$ (SNU)	$^{71}\mathrm{Ga}\rightarrow^{71}\mathrm{Ge}$ (SNU)	$^{8}\mathrm{B}$ ν flux ($10^6\mathrm{cm}^{-2}\mathrm{s}^{-1}$)
Homestake[3]	$2.56 \pm 0.16 \pm 0.16$	—	—
GALLEX[4]	—	$77.5 \pm 6.2^{+4.3}_{-4.7}$	—
GNO[5]	—	$65.8^{+10.2+3.4}_{-\ 9.6-3.6}$	—
SAGE[6]	—	$67.2^{+7.2+3.5}_{-7.0-3.0}$	—
Kamiokande[7]	—	—	$2.80 \pm 0.19 \pm 0.33^{\dagger}$
Super-Kamiokande[8]	—	—	$2.32 \pm 0.03^{+0.08\dagger}_{-0.07}$
SNO[9]	—	—	$1.75 \pm 0.07^{+0.12}_{-0.11} \pm 0.05^{\ddagger}$
J.N. Bahcall *et al.*[1]	$7.6^{+1.3}_{-1.1}$	128^{+9}_{-7}	$5.05(1.00^{+0.20}_{-0.16})$
S. Turck-Chieze *et al.*[2]	7.44 ± 0.96	127.8 ± 8.6	4.95 ± 0.72

† Flux measured via νe elastic scattering.

‡ Flux measured via the charged-current reaction.

The Homestake chlorine experiment was the first attempt to observe solar neutrinos. Initial results obtained in 1968 showed no events above backgroud with upper limit of the solar-neutrino flux of 3 SNU [10]. After introduction of an improved electronics system which discriminates signal from background by measuring the rise time of the pulses from proportional counters, finite solar-neutrino flux has been observed since 1970. The solar-neutrino capture rate shown in Table 2 is a combined result of 108 runs between 1970 and 1994 [3]. It is only about 1/3 of the BP2000 prediction [1].

GALLEX presented the first evidence of *pp* solar-neutrino observation in 1992 [11]. Here also, the observed capture rate is significantly less than the SSM prediction. SAGE initially reported very low capture rate, $20^{+15}_{-20} \pm 32$ SNU, with a 90% confidence-level upper limit of 79 SNU [12]. Later, SAGE observed similar capture rate to that of GALLEX [13]. Both

GALLEX and SAGE groups tested the overall detector response with intense man-made ^{51}Cr neutrino sources, and observed good agreement between the measured ^{71}Ge production rate and that predicted from the source activity, demonstrating the reliability of these experiments. The GALLEX Collaboration formally finished observations in early 1997. Since April, 1998, a newly defined collaboration, GNO (Gallium Neutrino Observatory) resumed the observations.

3.2 Kamiokande and Super-Kamiokande: Kamiokande and Super-Kamiokande are real-time experiments utilizing νe scattering

$$\nu_x + e^- \rightarrow \nu_x + e^- \tag{5}$$

in a large water-Čerenkov detector (Kamiokande and Super-Kamiokande in Japan). It should be noted that the reaction Eq. (5) is sensitive to all active neutrinos, $x = e$, μ, and τ. However, the sensitivity to ν_μ and ν_τ is much smaller than the sensitivity to ν_e, $\sigma(\nu_e e) \approx 7\sigma(\nu_{\mu,\tau} e)$. The solar-neutrino flux measured via νe scattering is deduced assuming no neutrino oscillations.

These experiments take advantage of the directional correlation between the incoming neutrino and the recoil electron. This feature greatly helps the clear separation of the solar-neutrino signal from the background. Due to the high thresholds (7 MeV in Kamiokande and 5 MeV at present in Super-Kamiokande) the experiments observe pure ^{8}B solar neutrinos because *hep* neutrinos contribute negligibly according to the SSM.

The Kamiokande-II Collaboration started observing the ^{8}B solar neutrinos at the beginning of 1987. Because of the strong directional correlation of νe scattering, this result gave the first direct evidence that the Sun emits neutrinos [14](no directional information is available in radiochemical solar-neutrino experiments). The observed solar-neutrino flux was also significantly less than the SSM prediction. In addition, Kamiokande-II obtained the energy spectrum of recoil electrons and the fluxes separately measured in the daytime and nighttime. The Kamiokande-II experiment came to an end at the beginning of 1995.

Super-Kamiokande is a 50-kton second-generation solar-neutrino detector, which is characterized by a significantly larger counting rate than the first-generation experiments. This experiment started observation in April 1996. The average solar-neutrino flux is smaller than, but consistent with, the Kamiokande-II result. The flux measured in the nighttime is slightly higher than the flux measured in the daytime, but it is only a 1.3σ effect [8]. Super-Kamiokande also observed the recoil-electron energy spectrum. Initially, its shape showed an excess at the high-energy end (> 13 MeV) compared to the SSM expectation, though its statistical significance was not very high [15]. More recent results indicate that the high-energy excess is reduced with the accumulation of statistics and it is concluded that the recoil electron spectrum is consistent with no spectral distortion [8].

3.3 SNO: In 1999, a new realtime solar-neutrino experiment, SNO (Sudbury Neutrino Observatory) started observation. This experiment uses 1000 tons of ultra-pure heavy water (D_2O) contained in a spherical acrylic vessel, surrounded by ultra-pure H_2O shield. SNO measures ^{8}B solar neutrinos via the reactions

$$\nu_e + d \rightarrow e^- + p + p \tag{6}$$

and

$$\nu_x + d \rightarrow \nu_x + p + n \ , \tag{7}$$

as well as νe scattering, Eq. (5). The charged-current (CC) rection, Eq. (6), is sensitive only to electron neutrinos, while the neutral-current (NC) rection, Eq. (7), is sensitive to all active neutrinos.

The Q-value of the CC reaction is -1.4 MeV and the electron energy is strongly correlated with the neutrino energy. Thus, the CC reaction provides an accurate measure of the shape of the ^{8}B solar-neutrino spectrum. The contributions from the CC reaction and νe scattering can be distinguished by using different cos $\theta_\odot$ distributions where $\theta_\odot$ is the angle with respect to the direction from the Sun to the Earth. While the νe scattering events have a strong forward peak, CC events have an approximate angular distribution of $1 - 1/3 \cos\theta_\odot$.

The threshold of the NC reaction is 2.2 MeV. In the pure D_2O, the signal of the NC reaction is neutron capture in deuterium, producing γ-rays with a total energy of 6.25 MeV. In this case, capture efficiency is low and the deposited energy is close to the detection threshold of 5 MeV. In order to enhance both the capture efficiency and the total γ-ray energy (8.6 MeV), 2.5 tons of NaCl is added to the heavy water in the second phase of the experiment. In addition, installation of discrete ^{3}He neutron counters is planned for the NC measurement in the third phase.

Recently, the SNO Collaboration published the initial results on the measurement of the ^{8}B solar-neutrino flux via CC reaction [9]. The electron energy spectrum and the $\cos\theta_\odot$ distribution have also been measured. The spectral shape of the electron energy is consistent with the expectations for no oscillation.

SNO also measured the ^{8}B solar-neutrino flux via νe scattering. Though the latter result has poor statistics yet, it is consistent with the high-statistics Super-Kamiokande result. Thus, the SNO group compared their CC result with Super-Kamiokande's νe scattering result, and obtained evidence of an active non-ν_e component in the solar-neutrino flux, as further described below.

3.4 Comparison of Experimental Results with Solar-Model Predictions: It is clear from Table 2 that the results from all the solar-neutrino experiments indicate significantly less flux than expected from the BP2000 SSM [1] and the Turck-Chieze et al. solar model [2].

There has been a consensus that a consistent explanation of all the results of solar-neutrino observations is unlikely within the framework of astrophysics using the solar-neutrino spectra given by the standard electroweak model. Many authors made solar model-independent analyses constrained by the observed solar luminosity [16–20], where they attempted to fit the measured solar-neutrino capture rates and ^{8}B flux with normalization-free, undistorted energy spectra. All these attempts only obtained solutions with very low probabilities.

The data therefore suggest that the solution to the solar-neutrino problem requires nontrivial neutrino properties.

4. Implications of the SNO and Super-Kamiokande Results: Evidence for Solar Neutrino Oscillations:

Denoting the ^{8}B solar-neutrino flux obtained by the SNO CC measurement as $\phi^{\rm CC}_{\rm SNO}(\nu_e)$ and that obtained by the Super-Kamiokande νe scattering as $\phi^{\rm ES}_{\rm SK}(\nu_x)$, $\phi^{\rm CC}_{\rm SNO}(\nu_e) = \phi^{\rm ES}_{\rm SK}(\nu_x)$ is expected for the standard neutrino physics. However, the data indicate

$$\phi^{\rm ES}_{\rm SK}(\nu_x) - \phi^{\rm CC}_{\rm SNO}(\nu_e) = (0.57 \pm 0.17) \times 10^6 \ \ {\rm cm}^{-2}{\rm s}^{-1} \ . \qquad (8)$$

The significance of the difference is $> 3\sigma$, implying direct evidence for the existence of a non-ν_e active neutrino flavor component in the solar-neutrino flux. A natural and most probable explanation of neutrino flavor conversion is neutrino oscillation. Note that both the SNO [9] and Super-Kamiokande [8] flux results were obtained by assuming the standard ^{8}B neutrino spectrum shape. This assumption is justified by the measured energy spectra in both of the experiments.

From the measured $\phi^{\rm CC}_{\rm SNO}(\nu_e)$ and $\phi^{\rm ES}_{\rm SK}(\nu_x)$, the flux of non-$\nu_e$ active neutrinos, $\phi(\nu_{\mu\tau})$, and the total flux of active ^{8}B solar neutrinos, $\phi(\nu_x)$, can be deduced:

$$\phi(\nu_{\mu\tau}) = (3.69 \pm 1.13) \times 10^6 \ \ {\rm cm}^{-2}{\rm s}^{-1} \qquad (9)$$

and

$$\phi(\nu_x) = (5.44 \pm 0.99) \times 10^6 \ \ {\rm cm}^{-2}{\rm s}^{-1} \ . \qquad (10)$$

Eq. (10) is a solar model-independent result and therefore tests solar models. It shows very good agreement with the ^{8}B solar-neutrino flux predicted by the BP2000 SSM [1] and that predicted by Turck-Chieze *et al.* model [2].

5. Global Analyses of the Solar Neutrino Data: A number of pre-SNO global analyses of the solar-neutrino data in terms of two neutrino oscillations yielded various solutions. For example, Bahcall, Krastev, and Smirnov [21] found at 99.7% confidence level eight allowed discrete regions in two-neutrino oscillation space. These are five solutions for active neutrinos (LMA, SMA, LOW, VAC, and Just So^2) and three separate

solutions for sterile neutrinos (SMA(sterile), VAC(sterile), and Just So^2(sterile)). LMA, SMA, LOW, VAC are abbreviations of large mixing angle, small mixing angle, low probability or low mass, and vacuum, respectively. The best-fit points for the five solutions for active neutrinos are shown below.

- LMA: $\Delta m^2 = 4.2 \times 10^{-5}$ eV^2, $\tan^2\theta = 0.26$
- SMA: $\Delta m^2 = 5.2 \times 10^{-6}$ eV^2, $\tan^2\theta = 5.5 \times 10^{-4}$
- LOW: $\Delta m^2 = 7.6 \times 10^{-8}$ eV^2, $\tan^2\theta = 0.72$
- Just So^2: $\Delta m^2 = 5.5 \times 10^{-12}$ eV^2, $\tan^2\theta = 1.0$
- VAC: $\Delta m^2 = 1.4 \times 10^{-10}$ eV^2, $\tan^2\theta = 0.38$.

For the three solutions for sterile neutrinos, the best-fit points are similar to the corresponding solutions for active neutrinos.

Immediately after the report of SNO's first result [9], many authors [22–25] presented the results of global analyses including the SNO's CC data. In most of these analyses, the total event rates from chlorine and gallium experiments, SNO's CC event rate, and Super-Kamioknade's day and night spectra are used. The total event rate from Super-Kamiokande is not used because it is not independent from the spectral data. The theoretical solar-neutrino fluxes are taken from BP2000 SSM [1].

A common feature of the analyses which include Super-Kamiokande's spectral data [8] are:

- The LMA solution is most favored.
- The LOW and VAC solutions are next or thirdly favored depending on the analysis detail.
- The SMA solution is a significantly less good solution than the LOW and VAC solutions.
- All other solutions generally give poor fits except that the VAC(sterile) solution sometimes gives as good a fit as the VAC or LOW solution.

It should be noted that all the favored solutions, LMA, LOW, and VAC, have large mixing angles.

6. Future Prospects: The SNO solar-neutrino measurement via CC reactions established solar-neutrino oscillations at $> 3\sigma$ level. The next step is to determine the solution uniquely. The forthcoming data from SNO and from new solar-neutrino experiments will provide important clues to discriminate the solutions.

Future SNO results will include the day-night flux asymmetry, more precise energy spectrum, and NC/CC ratio. SNO's expected day-night effect is substantially larger at the best-fit region of the LMA solution than at the best-fit region of the LOW solution. However, for both the LMA and LOW solutions, no spectrum distortion is expected. The SMA and VAC solutions will give detectable spectrum distortion. SNO's observation of solar-neutrino flux by NC reactions will give further evidence for neutrino oscillations into active neutrinos.

An important task of the future solar neutrino experiments is the measurement of monochromatic ^{7}Be solar neutrinos. If the VAC solution is correct, the flux of ^{7}Be neutrinos shows larger seasonal variations than the flux of ^{8}B neutrinos. In the LOW region, a strong day-night effect is expected. The ^{7}Be neutrino flux will be measured by a new experiment, Borexino, at Gran Sasso *via* νe scattering in 300 tons of ultra-pure liquid scintillator with a detection threshold as low as 250 keV. The Borexino experiment is expected to turn on in 2002.

KamLAND is an experiment similar to, but larger than Borexino. It is located at Kamioka, and 1000 tons of ultra-pure liquid scintillator is used. This experiment will also observe ^{7}Be neutrinos if the detection threshold can be lowered to a level similar to that of Borexino. However, one of the primary purposes of this experiment is the observation of oscillations of neutrinos produced by power reactors. The sensitivity region of KamLAND includes the LMA solution. Thus, the presently most-favored LMA solution may be proved or excluded by KamLAND. KamLAND is expected to turn on early in 2002.

References

1. J.N. Bahcall, M.H. Pinsonneault, and S. Basu, Astrophys. J. **555**, 990 (2001).
2. S. Turck-Chieze *et al.*, Astrophys. J. **555**, L69 (2001).
3. B.T. Cleveland *et al.*, Ap. J. **496**, 505 (1998).
4. W. Hampel *et al.*, Phys. Lett. **B447**, 127 (1999).
5. M. Altmann *et al.*, Phys. Lett. **B490**, 16 (2000).
6. J.N. Abdurashitov *et al.*, Phys. Rev. **C60**, 0055801 (1999).
7. Y. Fukuda *et al.*, Phys. Rev. Lett. **77**, 1683 (1996) [FUKUDA 96].

8. Y. Fukuda *et al.*, Phys. Rev. Lett. **86**, 5651 (2001).
9. Q.R. Ahmad *et al.*, Phys. Rev. Lett. **87**, 071301 (2001).
10. R. Davis, Jr. *et al.*, Phys. Rev. Lett. **20**, 1205 (1968).
11. P. Anselmann *et al.*, Phys. Lett. **B285**, 376 (1994).
12. A.I. Abazov *et al.*, Phys. Rev. Lett. **67**, 3332 (1991).
13. J.N. Abdurashitov *et al.*, Phys. Lett. **B328**, 234 (1994).
14. K.S. Hirata *et al.*, Phys. Rev. Lett. **63**, 16 (1989).
15. Y. Fukuda *et al.*, Phys. Rev. Lett. **82**, 2430 (1999).
16. N. Hata, S. Bludman, and P. Langacker, Phys. Rev. **D49**, 3622 (1994).
17. N. Hata and P. Langacker, Phys. Rev. **D52**, 420 (1995).
18. N. Hata and P. Langacker, Phys. Rev. **D56**, 6107 (1997).
19. S. Parke, Phys. Rev. Lett. **74**, 839 (1995).
20. K.M. Heeger and R.G.H. Robertson, Phys. Rev. Lett. **77**, 3720 (1996).
21. J.N. Bahcall, P.I. Krastev, and A.Yu. Smirnov, JHEP 05, 015 (2001).
22. G.L. Fogli *et al.*, `hep-ph/0106247`.
23. J.N. Bahcall, M.C. Gonzalez-Garcia, and C. Pena-Garay, JHEP 08, 014 (2001).
24. A. Bandyopadhyay *et al.*, `hep-ph/0106264`.
25. P.I. Krastev and A. Yu. Smirnov, `hep-ph/0108177`.